Journal of the National Cancer Center 5 (2025) 82–92

Contents lists available at ScienceDirect

Journal of the National Cancer Center

journal homepage: www.elsevier.com/locate/jncc

Short Communication

Integrated molecular characterization reveals the pathogenesis and therapeutic strategies of pulmonary blastoma ☆

He Tian [1,2,†], Zhenlin Yang [1,†], Junhui Yang [3,†], Ying Chen [4,†], Lin Li [5], Tao Fan [1], Tiejun Liu [1], Guangyu Bai [1], Yibo Gao [1,*], Jie He [1,*]

[1] *Department of Thoracic Surgery, National Cancer Center/National Clinical Research Center for Cancer/Cancer Hospital, Chinese Academy of Medical Sciences, Peking Union Medical College, Beijing, China*
[2] *Department of Respiratory Medicine, Fuwai Hospital, National Center for Cardiovascular Diseases, Chinese Academy of Medical Sciences & Peking Union Medical College, Beijing, China*
[3] *State Key Laboratory of Respiratory Disease, National Clinical Research Center for Respiratory Disease, Guangzhou Institute of Respiratory Health, the First Affiliated Hospital of Guangzhou Medical University, Guangzhou, China*
[4] *Department of Thoracic Surgery I, The Third Affiliated Hospital of Kunming Medical University (Yunnan Cancer Hospital, Yunnan Cancer Center), Kunming, China*
[5] *Department of Pathology, National Cancer Center/National Clinical Research Center for Cancer/Cancer Hospital, Chinese Academy of Medical Sciences, Peking Union Medical College, Beijing, China*

ARTICLE INFO

Keywords:
Pulmonary blastoma
Multi-omic profiling
Pathogenesis
Therapeutic strategies

ABSTRACT

Background: Pulmonary blastoma (PB) is a rare subtype of lung cancer. Currently, the underlying pathogenesis mechanisms of PB have not been fully illustrated, and the therapeutic approach for this entity is limited.

Methods: Whole-exome sequencing (WES), RNA sequencing, and DNA methylation profiling are applied to seven PB patients. Multi-omics data of pulmonary sarcomatoid carcinoma (PSC) and pituitary blastoma (PitB) from previous studies are invoked to illuminate the associations among PB and these malignacies.

Results: We portray the genomic alteration spectrum of PB and find that *DICER1* is with the highest alteration rate (86 %). We uncover that *DICER1* alterations, Wnt signaling pathway dysregulation and IGF2 imprinting dysregulation are the potential pathogenesis mechanisms of PB. Moreover, we reveal that the integrated molecular features of PB are distinct from PSC, and the molecular characteristics of PB are more similar to PitB than to PSC. Pancancer analysis show that the tumor mutation burden (TMB) and leukocyte fraction (LF) of PB are low, while some cases are positive for PD-L1 or have CD8-positive focal areas, implying the potential applicability of immunotherapy in selected PB patients.

Conclusion: This study depicts the integrated molecular characteristics of PB and offers novel insights into the pathogenesis and therapeutic strategies of PB.

1. Introduction

Pulmonary blastoma (PB), a rare branch of lung cancer, consistutes < 0.1 % of resected lung cancers.[1-3] PB is most common in middle-aged people, and the patients usually present with non-specific clinical syptoms similar to lung cancer. The 5- and 10-year survival rates of PB were 58.2 % and 48.5 %, repectively.[1] In recent years, PB has received more attentions in both clinical practice and molecular oncology research.

Orthodoxly, PB is a biphasic tumor consisting of low-grade fetal adenocarcinoma/well-differentiated fetal adenocarcinoma (WDFA) and primitive mesenchymal stroma, according to the definition of the 5th edition of the World Health Organization (WHO) classification of thoracic tumors in 2021. Previous studies have identified several frequently mutated genes in PB, including *DICER1, CTNNB1, TP53*, and *EGFR*.[4-11] Pulmonary fetal adenocarcinoma is lung adenocarcinoma resembling the developing fetal lung in its pseudoglandular stage.[12] Although WDFA is defined as a subtype of fetal adenocarcinoma by WHO, it is considered as the monophasic variant of PB by many researchers.[4] This mainly derives from the similarities of pathological contexture and genetic features between WDFA and PB.[4,13] PB is a subtype of pulmonary

☆ Given his role as Editor in Chief, Jie He had no involvement in the peer-review of this article and has no access to information regarding its peer-review. Full responsibility for the editorial process for this article was delegated to Huan He.

* Corresponding authors.
E-mail addresses: gaoyibo@cicams.ac.cn (Y. Gao), hejie@cicams.ac.cn (J. He).

† These authors contributed equally to this work.

https://doi.org/10.1016/j.jncc.2024.12.001
Received 4 November 2023; Received in revised form 30 November 2024; Accepted 1 December 2024

Table 1
Clinicopathological characteristics of PB patients.[a]

Patient ID	Pa1	Pa2	Pa3	Pa4	Pa5	Pa6	Pa7
City	Beijing	Beijing	Beijing	Beijing	Kunming	Kunming	Kunming
Year of diagonsis	2005	2009	2009	2016	2019	2017	2016
Gender	Female	Male	Male	Female	Female	Male	Male
Age at diagnosis, years	46	50	40	47	25	67	43
Family history[b]	No	No	No	No	No	No	No
Smoking pack-year	0	0	40	0	0	40	9
Tumor location	LLL	RML+RUL	RML+RLL	RUL	RUL	RLL	RML
Tumor Size, cm	2.3 × 2.2 × 2	22×10×8	9 × 8*6	11×9×4	1.4 × 1.5 × 1.6	3 × 2.5 × 1	5 × 2×0.4
TNM Stage	pT1cN0M0	pT4N0M0	pT4N0M0	pT4N0M0	pT1bN0M0	pT2aN0M0	pT2bN2M0
	IA3	IIIA	IIIA	IIIA	IA2	IB	IIIA
Subtype	WDFA	CBPB	CBPB	CBPB	WDFA	CBPB	CBPB
Treatment	No	No	Chemo	Chemo	No	Chemo plus Immuno	Chemo
WES	T + N	T + N	T + N	T + N	T	T + N	T
RNA-seq	NA	T + N	T + N	T + N	T	T	T
Methylation	T	T + N	T + N	T + N	T	T + N	T

[a] All patients in this study received radical resection of PB.
[b] Refers to the immediate family members of the patient (including parents, siblings, and children) who have a history of malignancies.
Abbreviations: CBPB, classic biphasic pulmonary blastoma; Chemo, chemotherapy; Immuno, immunotherapy; LLL, left lower lung; N, matched normal lung sample; NA, not available; Pa, patient; RLL, right lower lung; RML, right middle lung; RUL, right upper lung; T, tumor sample; WDFA, well-differentiated fetal adenocarci noma; WES, whole exose sequencing.

sarcomatoid carcinoma (PSC), and is widely regarded as a disease related to *DICER1* mutation. Pleuropulmonary blastoma (PPB) is a malignancy of the *DICER1* syndrome, while it usually occurs in children and is now defined as a different entity with PB.[14]

Surgical resection is the mainstream treatment for PB currently, while other therapies are still in the cradle. Radical resection is proved to be a protective factor for the long-term survival of PB in the American cohort.[1,15,16] Radiotheray, chemotherapy, and targeted therapy have been reported effective in a few cases of PB;[17-19] therefore solid conclusions about their efficacy in PB are lacking. Moreover, the effectiveness of immunotherapy for PB is still underexplored. Generally, effective treatments for PB remain a burning unmet clinical need currently. Integrated molecular research on PB was highly constrained by the rarity of this disease and the limitation of profiling techniques, hampering the management of this entity.

This study faithfully recapitulates the multi-omic profile of seven PB patients and compares the molecular features among PB, PSC, and pituitary blastoma (PitB). We provide a comprehensive genomic alteration spectrum of PB and report that *DICER1* alterations, the Wnt signaling pathway dysregulation and IGF2 imprinting dysregulation are the potential pathogenesis mechanisms of PB. Moreover, we reveal that the integrated molecular features of PB are distinct from PSC, and the molecular characteristics of PB are more similar to PitB than to PSC. Pancacer analysis show that the tumor mutation burden (TMB) and leukocyte fraction (LF) of PB are low, while some cases are positive for PD-L1 or have CD8-positive focal areas, implying the potential applicability of immunotherapy in selected PB patients. Our findings offered novel insights into the pathogenesis and therapeutic strategies of PB.

2. Materials and methods

2.1. Patients and samples

Seven PB patients diagnosed from 2005 to 2019 were enrolled in our study, in which 4 patients underwent surgery at Cancer Hospital, the Chinese Academy of Medical Sciences, and the other 3 patients accepted surgery at The Third Affiliated Hospital of Kunming Medical University, Yunnan Cancer Hospital, Yunnan Cancer Center. Two independent pulmonary pathologists confirmed the diagnosis based on the 5th edition of the WHO classification of thoracic tumors. All PB patients accepted no treatment before surgery and were without other malignant conditions. The clinicopathological information of them was retrieved from the medical record system, and the tumor samples and paired normal lung tissues were retrospectively collected from the archive of the Department of Pathology. We applied whole-exome sequencing (WES), RNA-seq, and DNA methylation profiling to our PB cohort. Additionally, we introduced the data of PSC and PitB from previous studies[20-22] into our analysis. For PSC, the mutation data of 55 patients, the RNA-seq data of 14 patients, and the methylation data of 44 patients were utilized. For PitB patients, the mutation data of 11 patients and the methylation data of 8 patients were employed. The sample procession and sequencing data anlaysitic methods were detailed in the Supplemetary materials.

2.2. Statistics analysis

Statistical analysis was performed using Fisher's exact test for categorical variables, and the Wilcoxon test or Mann–Whitney U test was used for continuous variables. Statistical tests were performed in R (version 3.2.0). We regarded a two-tailed P-value < 0.05 as statistically significant.

3. Results

3.1. Study design and patient information

The workflow of this study was demonstrated in Fig. 1A. We applied multi-omic approaches to PB and invoked the PSC data and PitB data from previous studies[20-22] to explore the molecular characteristics associations among PB and these malignacies. Detailed clinical information of PB patients was in Table 1. Representative hematoxylin-eosin (HE) images of PB patients were shown in Fig. 1B. The median age of patients was 46 (range 25–67) years, and 57.1 % of patients were males. 42.9 % patients were tobacco users. The TNM stage was evaluated based on the 8th edition TNM stage criteria of lung cancer.[23] Totally four patients were identified as stage IIIA, and three patients were stage I. No patient was with a family history of PB.

3.2. Genomic alteration spectrum of PB

WES was performed on the DNA samples from seven PB patients to assess the genomic alterations globally. The average sequencing depth of tumor and normal samples were 223 × and 112 ×, respectively. The detailed sequencing quality information of WES and transcriptome were in Supplementary Table 1. In total, 809 nonsilent candidate somatic mutations were detected (Supplementary Table 2). The list of copy number

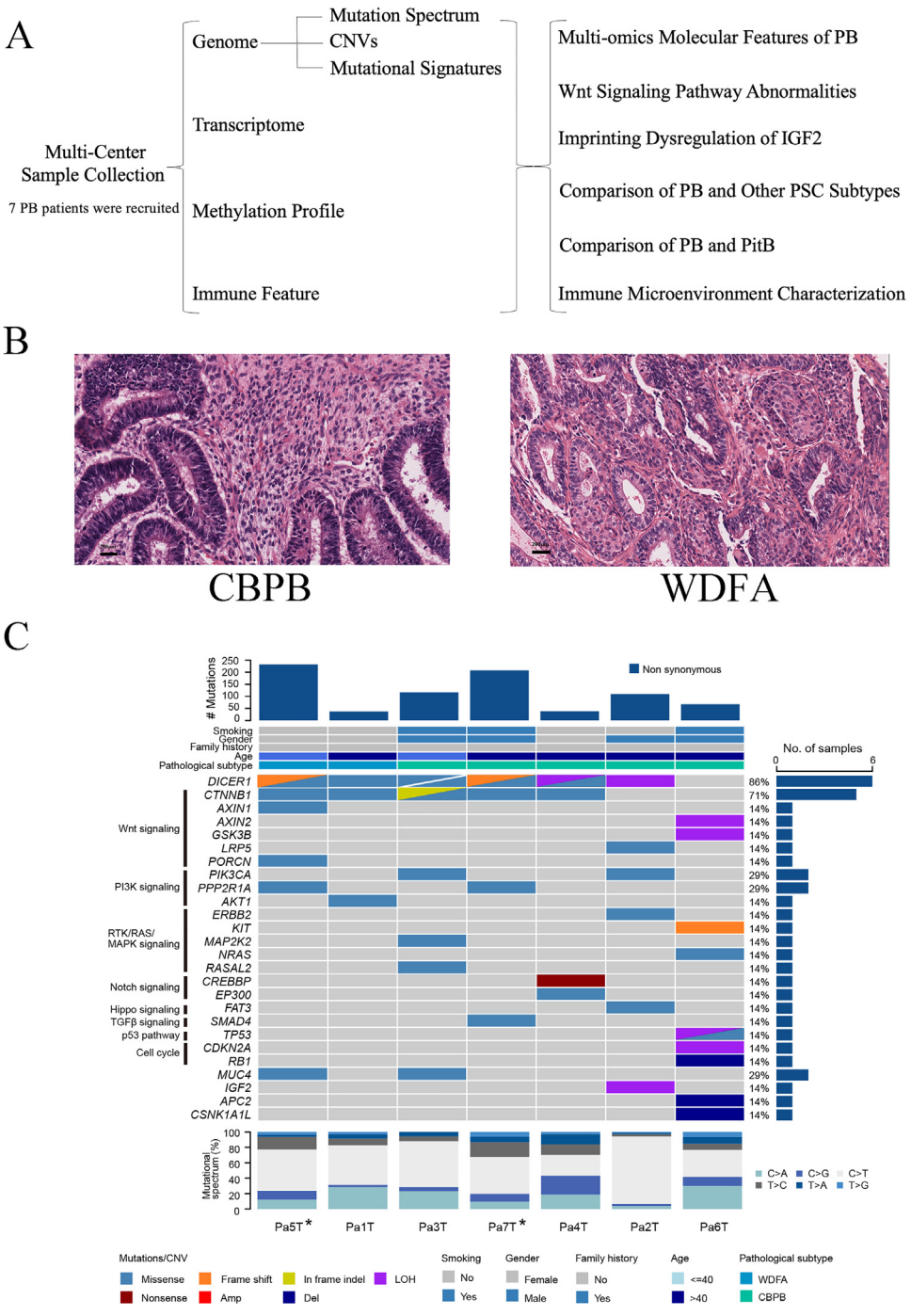

Fig. 1. Study design and PB alteration spectrum. (A) Workflow of this study. (B) Representative hematoxylin-eosin images of patients in our study. Scale bars, 200 μm. (C) Genomic alteration spectrum of PB. *, indicates patients without paired normal samples as controls in genomic alteration identification. Amp, amplification; CBPB, classic biphasic pulmonary blastoma; CNV, copy number variation; Del, deletion; LOH, loss of heterozygosity; Pa, patient; PB, pulmonary blastoma; PSC, pulmonary sarcomatoid carcinoma; PitB, Pituitary blastoma; T, tumor; WDFA, well-differentiated fetal adenocarcinoma.

variations (CNVs) and loss of heterozygosity (LOH) was provided in Supplementary Table 3. The contributions of 30 mutational signatures from the Catalogue of Somatic Mutations in Cancer (COSMIC) in each tumor was demonstrated in Supplementary Table 4. The genomic alteration spectrum of PB was displayed in Fig. 1C.

DICER1, encoding essential ribo-endonuclease processing pre-miRNAs into functional miRNAs,[24] was the gene with the highest alteration rate in our cohort (6/7, 86 %). Among the six patients with *DICER1* alterations, missense mutations were identified in five patients, affecting the amino acids Gly1809, Glu1813, and Asp1810, which were in the RNase IIIb domain and could cause the abnormal function of RNase IIIb in miRNA processing.[25] Moreover, there were four patients harboring two *DICER1* alterations,[11] suggesting the significance of "two-hit" mode of *DICER1* in PB pathogenesis. In addition, we identified exon 3 missense mutations of *CTNNB1* in five (5/7, 71 %) patients, which could affect the phosphorylation-mediated degradation of *β*-catenin and lead to aberrant stabilization of *β*-catenin, thus resulting in the abnormal activation of the Wnt signaling pathway.[26,27]

Wnt signaling pathway, PI3K signaling pathway, and RTK/RAS/MAPK signaling pathway were the pathways with frequent genomic alterations. In PI3K signling pathway, we identified *PIK3CA* and *AKT1* mutations in 28.6 % and 14.3 % of patients, respectively. The two missense mutations of *PIK3CA* both involved codon 1047, which is located within the kinase domain. The oncogenic *AKT1 E17K* mutation was identified

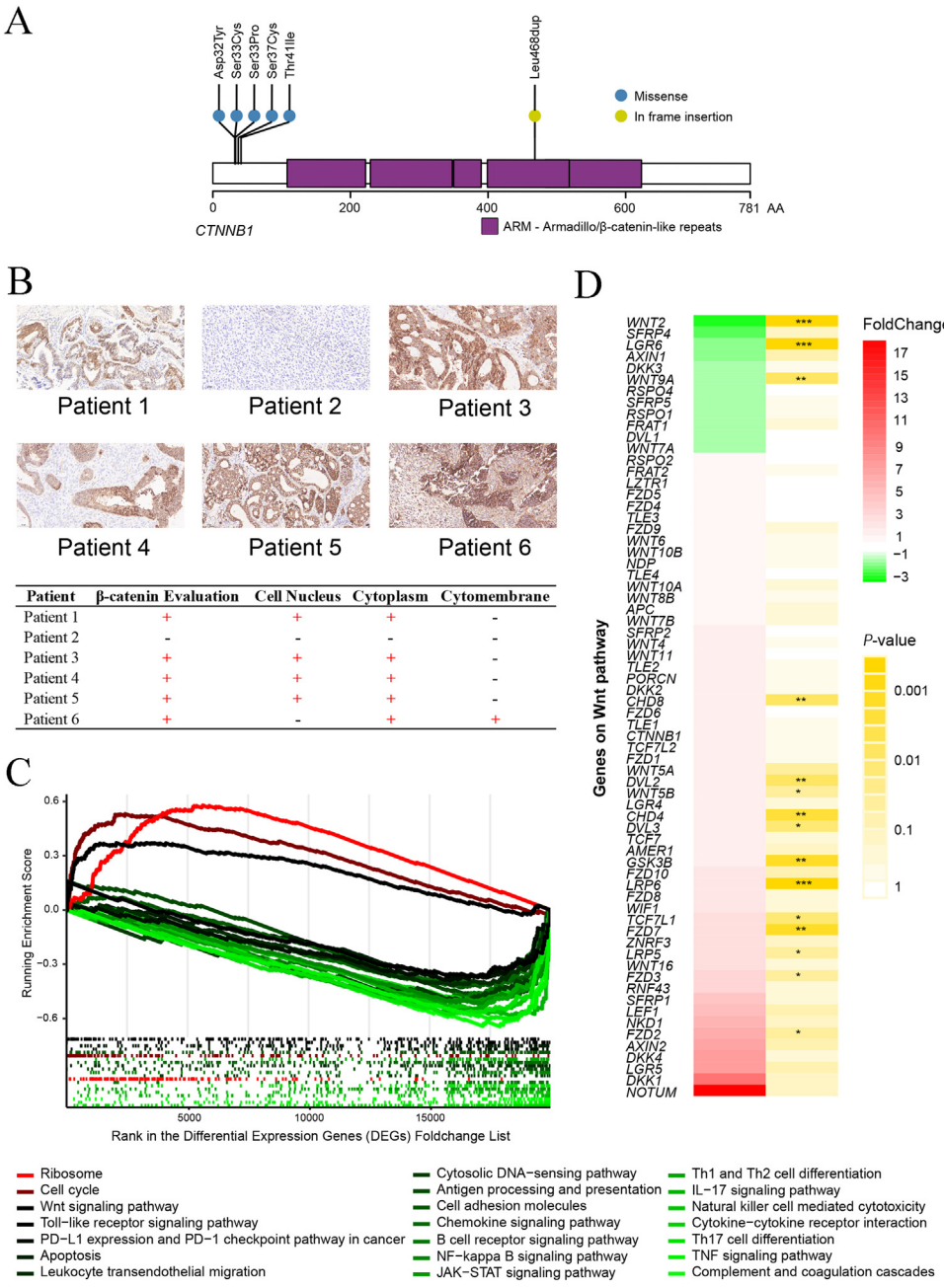

Patient	β-catenin Evaluation	Cell Nucleus	Cytoplasm	Cytomembrane
Patient 1	+	+	+	-
Patient 2	-	-	-	-
Patient 3	+	+	+	-
Patient 4	+	+	+	-
Patient 5	+	+	+	-
Patient 6	+	-	+	+

Fig. 2. Wnt signaling pathway dysregulation in PB. (A) CTNNB1 mutation distribution in PB. (B) Immunohistochemistry of β-catenin on PB. Upper panel, representative images of β-catenin expression. Lower panel, the pathological evaluation and the cellular location of β-catenin. For patient 7, formalin fixed paraffin embedded specimen was unavailable for immunohistochemistry analysis. (C) GSEA between the transcriptomic profiles of PB and normal lung tissues based on the fold change rank of all genes. (D) The expression of genes in Wnt signaling pathway. Foldchange represents the relative gene expression level of tumor samples over matched normal samples. *, $P < 0.05$; **, $P < 0.01$; and ***, $P < 0.001$. AA, amino acid; PB, pulmonary blastoma.

in one patient. Additionally, *TP53* missense mutation combined with LOH was identified in one patient, indicating the important roles of *TP53* in PB carcinogenesis; however, the mutation rate of *TP53* in PB was much lower than that of traditional lung cancer and other subtypes of PSC.[20,28,29]

3.3. Wnt signaling pathway dysregulation

CTNNB1, which encoded β-catenin, was the most frequently mutated genes in Wnt signling pathway. We identified *CTNNB1* mutations in 71.4% of patients, and the patients all harbored missense mutations involving exon 3 (Fig. 2A). The exon 3 of *CTNNB1* is a key region encoding serine-threonine phosphorylation sites for GSK3B, which could activate the phosphorylation and subsequent degradation of β-catenin in the cytoplasm under physiological conditions. The exon 3 mutations of *CTNNB1* would disrupt this degradation and lead to the nuclear accumulation of β-catenin.[26,30,31] Accordingly, immunohistochemistry (IHC) experiments demonstrated the aberrant nuclear accumulation of β-catenin in patient 1, 3, 4, and 5; all of whom were with *CTNNB1* exon 3 mutation (Fig. 2B).

Notably, β-catenin positive areas were also detected in patient 6, who was without detectable *CTNNB1* mutation. However, the β-catenin accumulation in this patient was only involved with the cytoplasm and cytomembrane (Fig. 2B), reinforcing the associations between *CTNNB1* exon 3 mutations and β-catenin nuclear accumulation. Additionally, we identified several genomic alterations of the Wnt signaling pathway in this patient, including *RSPO3* missense mutation, *APC2* deletion, *AXIN2* LOH, and *GSK3B* LOH (Supplementary Tables 2 and 3).

Further, we performed RNA-seq on the RNA samples from 6 PB patients. Totally, 23,437 genes were tested for differential expression between PB tumor and normal samples, and we performed gene set enrichment analysis (GSEA) of the Kyoto Encyclopedia of Genes and Genomes (KEGG) pathway based on the fold change rank of all genes. Several immune-related pathways and classical cancer-related pathways were significantly enriched, such as PD-L1 expression and PD-1 checkpoint pathway in cancer ($P = 0.0056$), B cell receptor signaling pathway

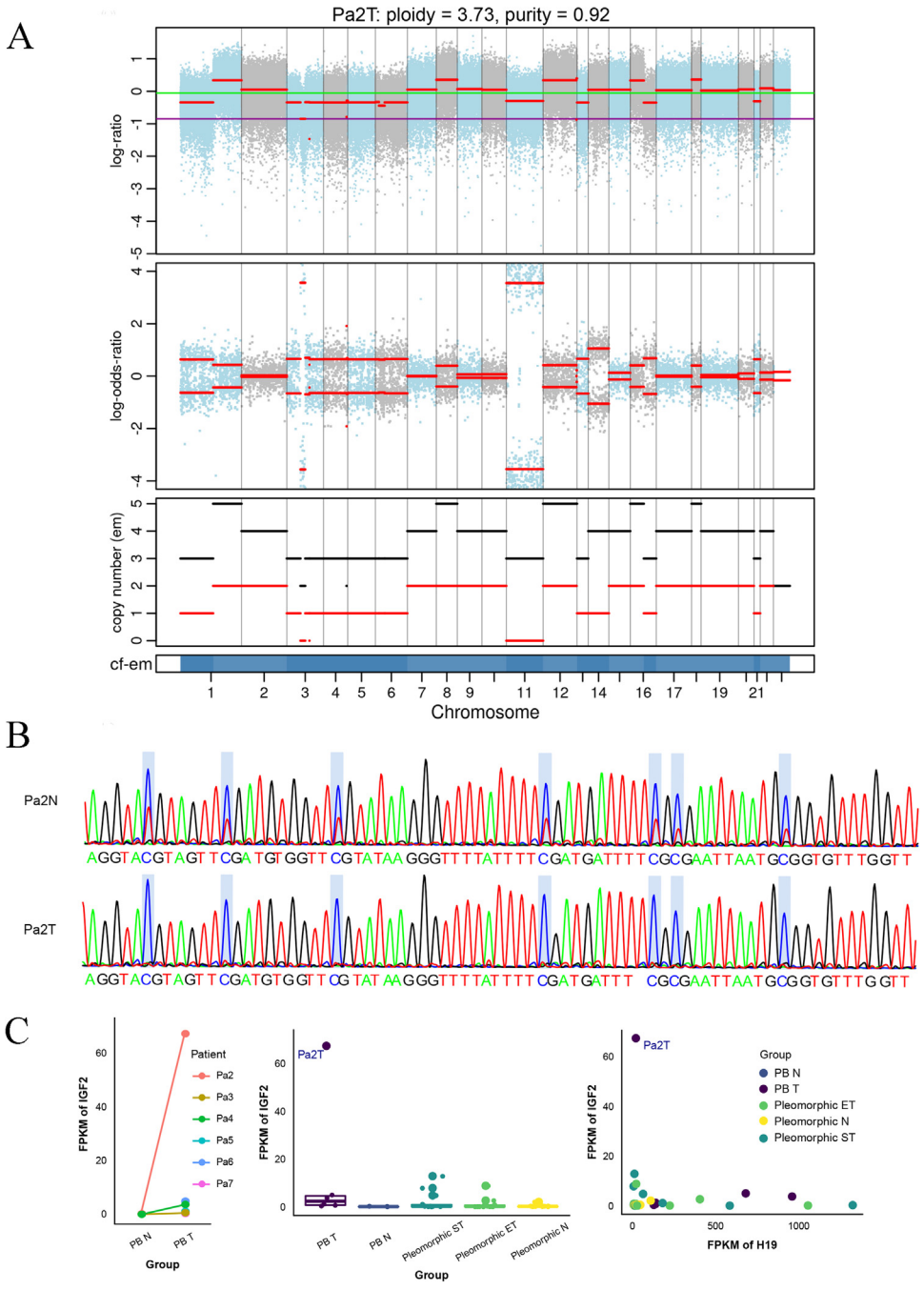

Fig. 3. IGF2 imprinting dysregulation in PB. (A) Somatic copy number variation of PB patient 2. First row, log ratio of tumor/normal read depth. The violet line represents the estimated value of log ratio when the copy number of the tumor is 2. The red line represents the patient's actual log ratio in chromosome. Second row, the log-odds ratio of the variant allele count in the tumor sample versus in the normal sample, which reflects the copy number discrepancy between alleles. Third row, the corresponding integer copy number calls. Black line, total copy number. Red line, minor copy number. Fourth row, cellular fraction. The light blue and dark blue represent the lower and the higher cellular fraction, respectively. (B) Bisulfite conversion and Sanger sequencing of patient 2. The sequencing range is chr11: 2,022,252–2,022,435, hg19. All the sequencing regions were within the IGF2-ICR1-H19 region. The upper and lower panel demonstrate the sequencing result of the matched normal sample and tumor sample of patient 2, respectively. The abnormal CpG sites were highlighted by blue background. (C) IGF2 expression pattern in PB and PSC. Left panel, IGF2 expression in PB. Middle panel, IGF2 expression in PB and PSC patients. Right panel, IGF2-H19 expression in PB and PSC patients. cf-em, cellular fraction; FPKM, fragments per kilobase of exon per million mapped fragments; Pa2N, matched normal sample of patient 2; Pa2T, tumor sample of patient 2; PB, pulmonary blastoma; PB N, matched normal samples of PB; PB T, tumor samples of PB; Pleomorphic ET, the epithelial component of the pleomorphic carcinoma; Pleomorphic N, matched normal samples of the pleomorphic carcinoma; Pleomorphic ST, the sarcomatoid component of the pleomorphic carcinoma, a subtype of PSC; PSC, pulmonary sarcomatoid carcinoma.

(P = 0.0009), Wnt signaling pathway (P = 0.0440), JAK-STAT signaling pathway (P = 0.0004), etc. (Fig. 2C). The detailed gene expression pattern of the Wnt signaling pathway is displayed in Fig. 2D. We observed that several genes of the R-spondin/LGR5/RNF43 module, including RNF43, LGR5, and ZNRF3, were over-expressed in PB tumor samples, indicating that the R-spondin/LGR5/RNF43 module dysfunction might play important roles in the Wnt signaling dysregulation of PB.

3.4. *IGF2 imprinting dysregulation in PB*

We found that no *CTNNB1* alteration was detected in patient 2, who was also negative in β-catenin IHC staining, indicating that molecular events other than Wnt signaling dysregulation were involved in the tumorigenesis (Fig. 1C and Fig. 2B). We illustrated the CNV and LOH detail of 5 PB patients with matched normal samples in Fig. 3A (patient 2) and Supplementary Fig. 1A (patients 1, 3, 4, and 6). The total copy number of patient 2 was >2, and the copy number discrepancy between alleles in chromosome 11 was more significant than that in other chromosomes (Fig. 3A and Supplementary Fig. 1B), indicating that LOH occurred in the chromosome region. This region affected an imprinted gene cluster at 11p15.5, where the paternal allele and the maternal allele expressed IGF2 and H19, respectively.[32] The IGF2-H19 expression is highly influenced by epigenetic mechanisms, primarily DNA methylation, and the binding of CCCTC-binding factor (CTCF) to the imprinting control region (ICR). Bisulfite conversion and Sanger sequencing revealed homozygous hypermethylation of ICR in the tumor sample of patient 2 (Fig. 3B), indicating that the LOH caused paternal uniparental polyploidy, which could result in aberrant IGF2 overexpression. To further validate the loss of imprinting of IGF2, we compared the expression level

of IGF2 among PB, pleomorphic carcinoma, and normal lung tissues, and found that the IGF2 expression of the tumor sample from patient 2 was significantly higher than that of other samples (Fig. 3C). In addition, we observed extremely high IGF2 expression combined with low H19 expression in the tumor of patient 2 (Fig. 3C). Taken together, the aberrant imprinting at the locus might be the driver alterations in the tumorigenesis of PB.

3.5. Differences in the molecular characteristics between PB and PSC

PB was classified as a subtype of PSC by the 5th edition of the WHO Classification of Thoracic Tumors in 2021, and we introduced the multi-omic data of PSC samples, including pleomorphic carcinoma and carcinosarcoma, from a previous study[20] into our analysis to depict the differences of the molecular characteristics among different subtypes of PSC. The detailed information of PSC samples we employed was in Supplementary Tables 8 and 9. Compared to other subtypes of PSC, PB was featured with significantly higher mutation frequencies of *DICER1, CTNNB1*, and Wnt signaling pathways. In contrast, the mutation rates of *TP53* and RTK/RAS/MAPK signaling pathways were lower in PB (Fig. 4A). The unsupervised clustering of the transcriptomic data demonstrated that PB tumor samples were well-distinguished from the pleomorphic PSC subtype, reinforcing the unique characteristics of PB (Fig. 4B). GSEA enriched several immune-related pathways between the transcriptomic profiles of PB and other subtypes of PSC, such as the natural killer cell-mediated cytotoxicity pathway and the antigen processing & presentation pathway (Fig. 4C). Further, we compared the DNA methylation profiles of PB and the other subtypes of PSC (Fig. 4D), where PB manifested distinct methylation traits compared with the other PSC subtypes. Multiple immune-related terms, classical cancer-related terms, and epigenetic-related terms were enriched by GSEA between the DNA methylation profiles of PB and other subtypes of PSC. Notably, the Wnt signaling pathways were also significantly enriched ($P < 0.01$), emphasizing its significance in PB (Fig. 4E).

3.6. Affinities between PB and PitB

PitB is a rare and lethal pediatric intracranial tumor[33] driven by *DICER1* mutations.[21,22,34] Histologically, PitB and PB are blastomas deriving from different organs. We depicted the association of the molecular features between the two malignancies. The detailed information of PitB samples we employed was in Supplementary Table 8. Generally, we observed high *DICER1* mutation rates in both PitB (90.9 %, $n = 11$) and PB (71.4 %, $n = 7$). We noticed that over half of the *DICER1* mutations in PB occurred in the RNase IIIa and IIIb domains. Although this region harbored several *DICER1* mutations in PitB, most *DICER1* mutations in PitB are scattered in other regions. For both PB and PitB, all the *DICER1* missense mutations were in the RNase IIIa and IIIb domains. Some PitB *DICER1* mutations (Arg509Ter, Arg676Ter, and Tyr793Ter) were nonsense mutations, while we did not detect nonsense *DICER1* mutations in PB. Compared to PB, many *DICER1* mutations in PitB were not located in any functional domain (Lys429AlafsTer47, Tyr793Ter, Asn1093Ter, Ser1179ThrfsTer12, and Asp1437MetfsTer16) (Fig. 5A and Supplementary Table 5). Next, we summarized the methylation features of PB, PitB, and PSC (Fig. 5B) and evaluated the similarity among the DNA methylation profiles of these malignancies by calculating the Euclidean distance. As shown in Fig. 5C and Supplementary Table 6, the similarity between PB and PitB was significantly higher than that between PB and PSC ($P = 7.2 \times 10^{-16}$), indicating the affinities between PB and PitB. GSEA between the DNA methylation profiles of PB and PitB revealed the enrichment of several immune-related terms and classical cancer-related terms, such as the T cell activation and Ras protein signal transduction. Moreover, the lung development term ($P < 0.01$) and the endocrine system development term ($P < 0.01$) were enriched, indicating the organ-specific features of PB and PitB despite their affinities (Fig. 5D).

3.7. Immune microenvironment features of PB

The introduction of immunotherapy has revolutionized the treatment paradigm of lung cancer, and the tumor immune microenvironment (TIME) is critical to the efficacy of immune checkpoint inhibitors (ICIs) .[35] Tumor mutation burden (TMB) and leukocyte fraction (LF) were reported to be predictive biomarkers for ICIs. Therefore, to further explore the feasibility of immunotherapy in PB, we performed pan-cancer TMB and LF analysis. As shown in Fig. 6A and Supplementary Table 6, PB was out of the top TMB cancer types. The average TMB of PB was 2.77 per megabase, lower than that of lung adenocarcinoma (LUAD, $P = 0.037$), lung squamous cell carcinoma (LUSC, $P = 0.001$), and PSC ($P = 0.077$). Both PB and PitB belonged to the cancer types with very low LF (Fig. 6B and Supplementary Table 7). The LF of PB was significantly lower than that of LUAD ($P = 0.001$), LUSC ($P = 0.004$), and PSC ($P = 0.001$). These results indicated that patients with PB might not be perfect beneficiaries for ICIs.

In addition, we performed IHC of PD-L1 and CD8 on our PB cohort. Patient 1 was positive for PD-L1 staining (tumor proportion score [TPS] = 1 %, combined positive score [CPS] = 2), and CD8-positive focal areas were detected in patients 1, 5, and 6 (Fig. 6C and D, Supplementary Fig. 2A and B). These results suggested that some PB patients, such as patient 1 and patient 6, might benefit from immunotherapy; however, further investigation is required.

4. Discussion

The history of PB can be traced back to 1965,[36] but our mastery of its nature and treatment is insufficient. Here, we portrayed PB's multi-omic profile and compared its molecular features with those of other subtypes of PSC and PitB. Our findings offered novel insights into PB's pathogenesis and therapeutic approaches.

DICER1 alteration, of great significance in cancer biology,[24] is a widely-accepted feature of pleuropulmonary blastoma,[9,37] and has been reported in diverse malignant diseases originating in other organs, such as PitB and pineoblastoma.[22,38] In our study, we observed that *DICER1* was the gene with the highest alteration rate, and the "two-hit" mode of *DICER1* might play an important role in the pathogenesis of PB. Although *DICER1* mutation has been reported in adult-onset PB previously,[8,11] we provided a comprehensive description in a relatively larger cohort. Moreover, we are looking forward to future resutls of comparing PB with other *DICER1*-associated adult-type malignancies, since these comparisions will also advance our recognation about the role *DICER-1* alteration played in PB.

Wnt signaling aberrant activation has been reported in multiple blastomas originating from different organs, including pancreatoblastoma,[39] hepatoblastoma,[40-42] and pituitary blastoma.[22] In our study, *CTNNB1* mutations were identified in 71.43 % (5/7) PB patients, all harboring *CTNNB1* exon 3 missense mutation, and were with β-catenin nuclear aberrant accumulation. Notably, we observed one patient who did not harbor *CTNNB1* mutation, and the β-catenin accumulation only occurred in the cytoplasm and the cytomembrane, reinforcing the effect of *CTNNB1* exon 3 mutations. It is notable that we detected *RSPO3* missense mutation, *APC2* deletion, *AXIN2* LOH, and *GSK3B* LOH in patient 6. *RSPO3* belongs to the R-spondin family, the enhancer of the Wnt signaling pathway,[43] while *APC2, AXIN2*, and *GSK3B* were members of the β-catenin destruction complex.[44] This suggests that the malfunction of these regulators might explain the aberrant expression of β-catenin. Moreover, the Wnt signaling pathway was significantly enriched in the GSEA analysis based on the differential expression of genes between PB tumors and normal lung tissues. Generally, aberrant Wnt signaling pathway activation might be an important molecular mechanism underlying the pathogenesis of PB.

In patient 2 of our cohort, no β-catenin accumulation was detected by IHC, indicating that other molecular mechanisms were involved in the tumorigenesis. We observed IGF2 imprinting dysregulation and

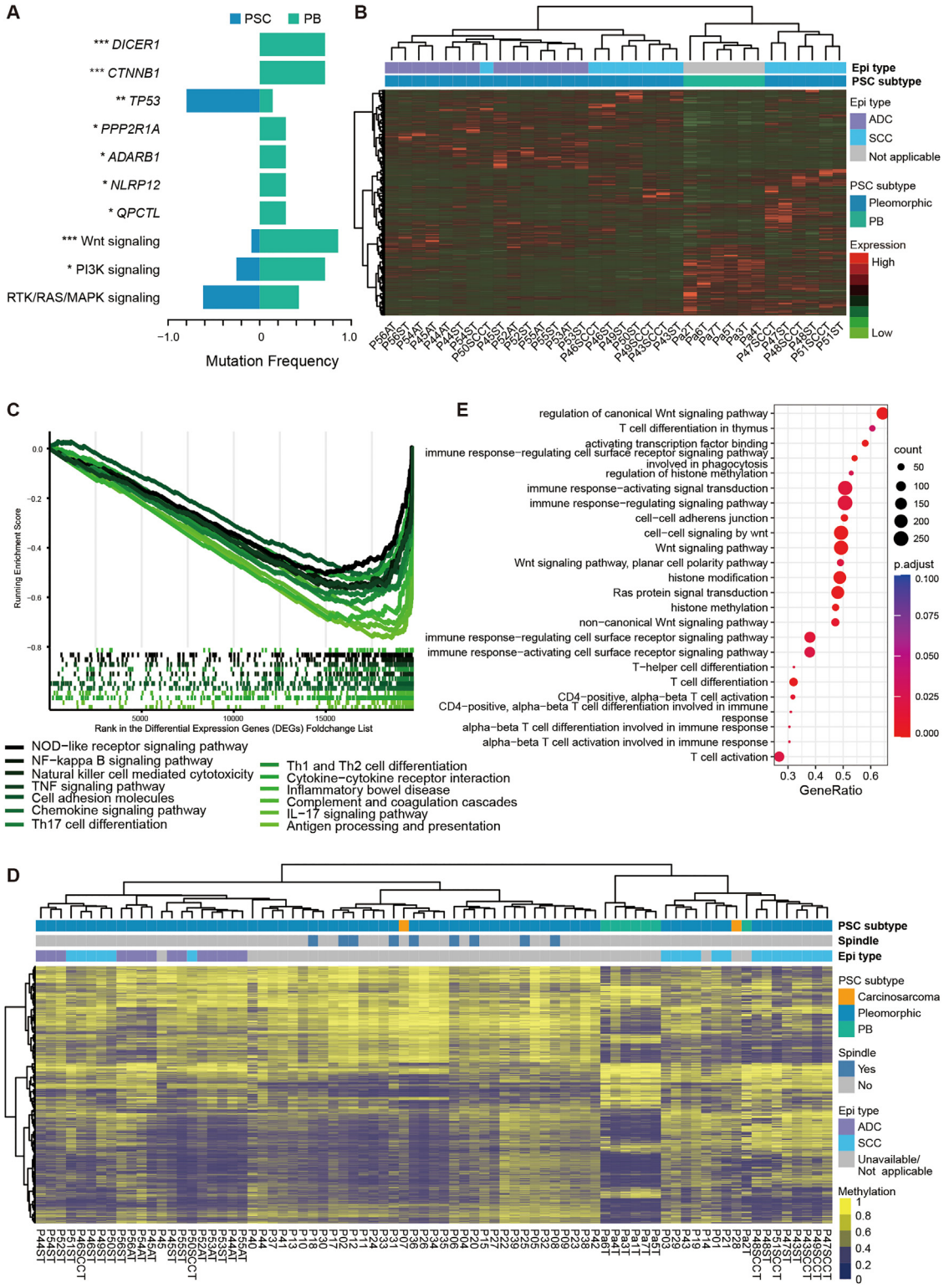

Fig. 4. Differences in the molecular characteristics between PB and PSC. (A) The mutation frequencies of representative genes and pathways in PB and PSC. Fisher's exact test was applied. *, $P < 0.05$; **, $P < 0.01$; ***, $P < 0.001$. About genes analyzed within Wnt, PI3K and RAS/MAPK pathway, PI3K signaling: PIK3CA, PPP2R1A, AKT1, PTEN, AKT3; Wnt signaling: CTNNB1, AXIN1, AXIN2, GSK3B, LRP5, PORCN; RTK/RAS/MAPK signaling: ERBB2, KIT, MAP2K2, NRAS, RASAL2, EGFR, KRAS, MET, BRAF, NF1. (B) Unsupervised clustering based on the transcriptomic data of PB and pleomorphic carcinoma. (C) GSEA between the transcriptomic profiles of PB and PSC based on the fold change rank of all genes. (D) Unsupervised clustering based on the DNA methylation profiles of PB and PSC. (E) GSEA between the DNA methylation profiles of PB and PSC based on the *P*-values of all CpGs. ADC, adenocarcinoma; AT, the adenocarcinoma of the epithelial component of the pleomorphic carcinoma; Epi type, epithelial type; PB, pulmonary blastoma; PSC, pulmonary sarcomatoid carcinomaSCC, squamous cell carcinoma. ST, the sarcomatoid component of the pleomorphic carcinoma; SCCT, the squamous cell carcinoma component of the pleomorphic carcinoma.

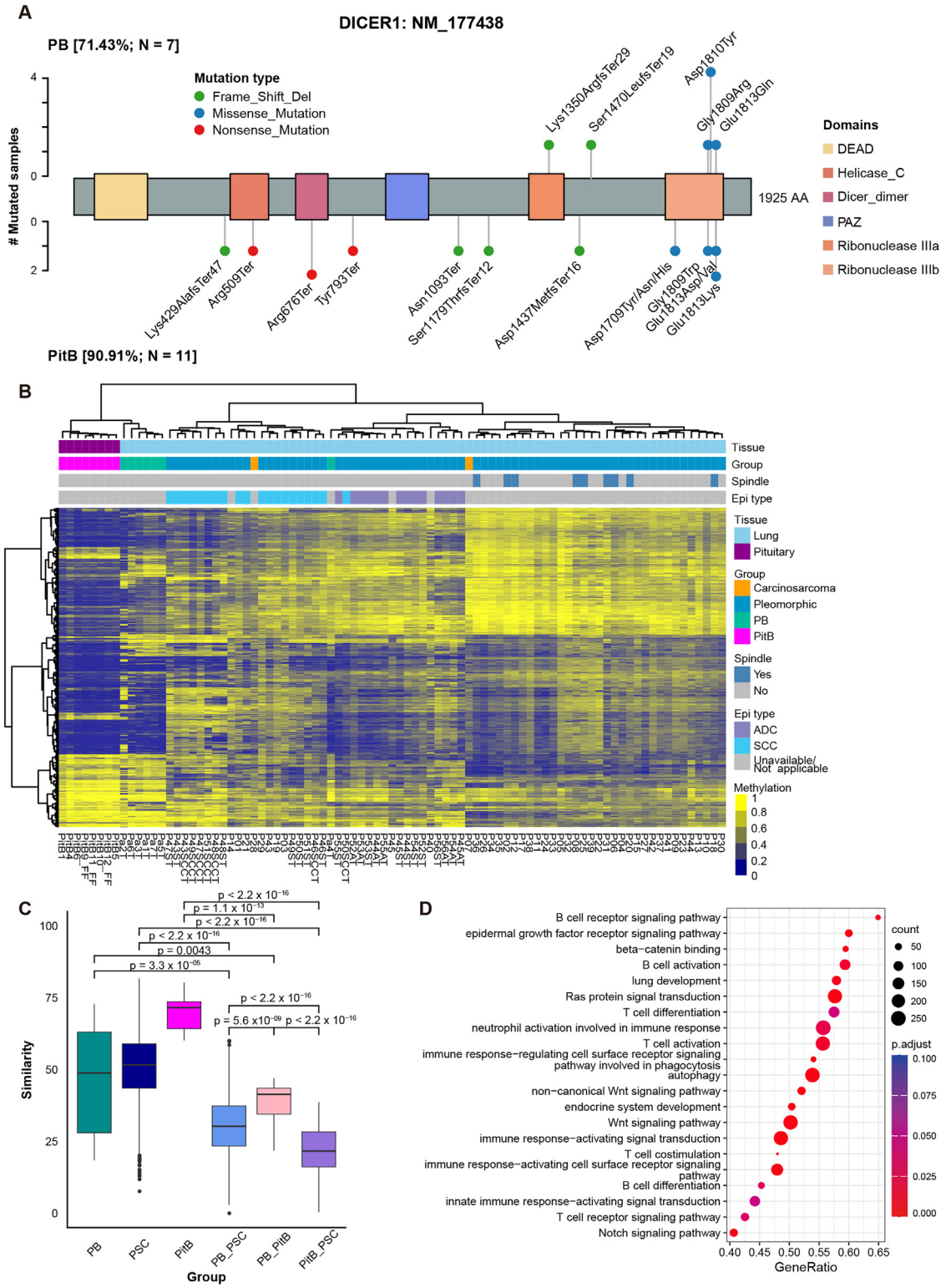

Fig. 5. Affinities between PB and PitB. (A) DICER1 mutation distribution in PB and PitB. (B) Unsupervised clustering based on the DNA methylation profiles of PB, PitB, and PSC. (C) Boxplots show the Euclidean distance-based similarities between each two pair of PB, PSC and PitB. Center line, median; box limits, upper and lower quartiles; whiskers, 1.5 × interquartile range; points, outliers. The Euclidean distance-based similarities were compared using the Wilcoxon test. (D) GSEA between the DNA methylation profiles of PB and PitB based on the *P*-value of all CpGs. ADC, adenocarcinoma; AT, the adenocarcinoma of the epithelial component of the pleomorphic carcinoma; Epi type, epithelial type; DEAD, DEAD/DEAH box helicase; Dicer_dimer: Dicer dimerisation domain; Helicase_C, Helicase conserved C-terminal domain; PAZ, PAZ domain; PB, pulmonary blastoma; PitB, Pituitary blastoma; PSC, pulmonary sarcomatoid carcinoma; Ribonuclease III, Ribonuclease III domain; SCC, squamous cell carcinoma; SCCT, the squamous cell carcinoma component of the pleomorphic carcinoma; ST, the sarcomatoid component of the pleomorphic carcinoma.

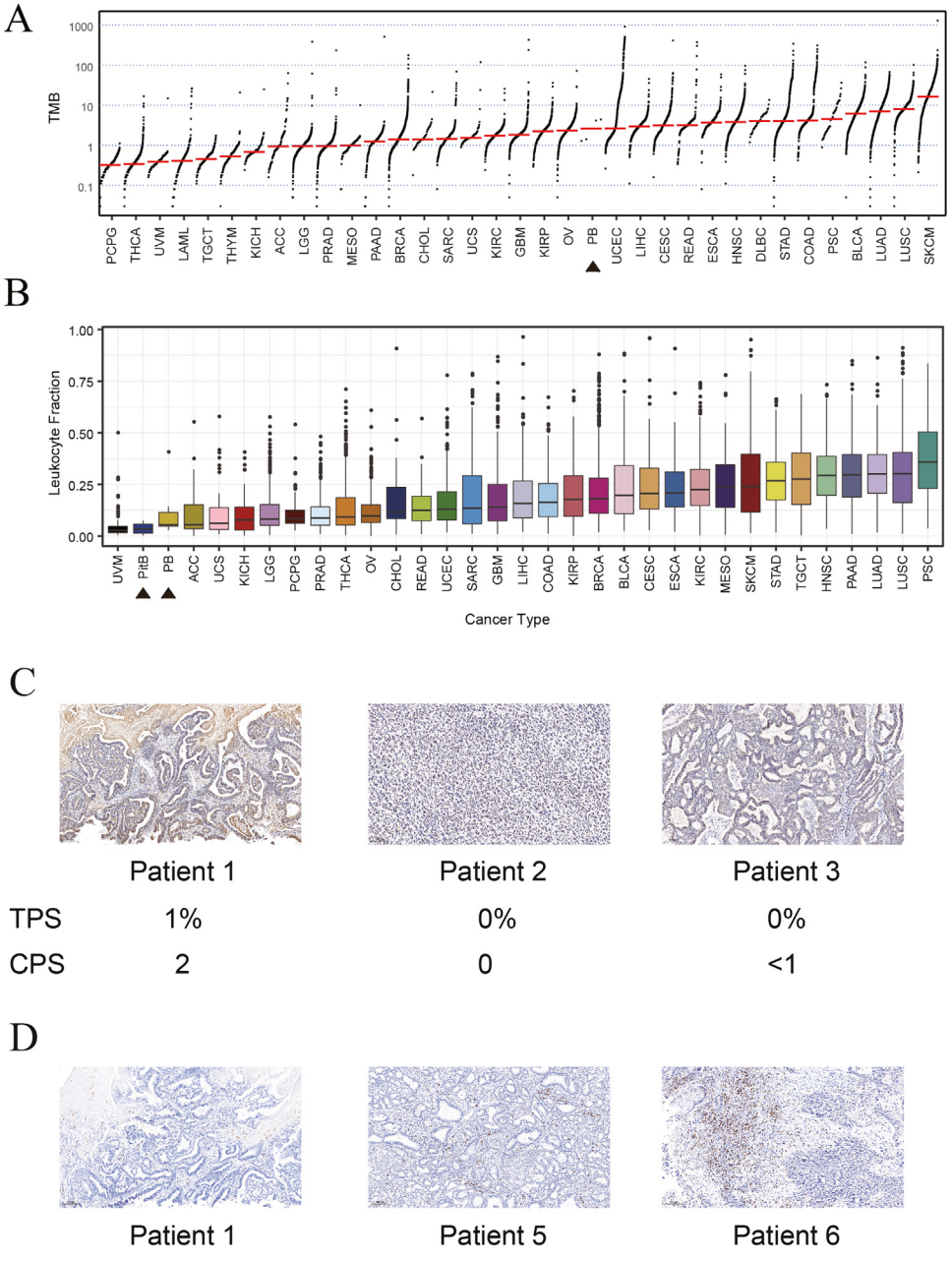

Fig. 6. Immune microenvironment characterization of PB. (A) Pan-cancer analysis of TMB in PB, PSC, and TCGA tumor types. (B) Pan-cancer analysis of leukocyte fraction in PB, PitB, PSC, and TCGA tumor types. (C) Representative images of PD-L1 staining in PB. (D) Representative images of CD8 staining in PB. Scale bars, 100 μm. ACC, adrenocortical cancer; BLCA, bladder urothelial carcinoma; BRCA, breast invasive carcinoma; CESC, cervical & endocervical cancer; CHOL, cholangiocarcinoma; COAD, colon adenocarcinoma; CPS, combined positive score; DLBC, diffuse large B-cell lymphoma; ESCA, esophageal carcinoma; GBM, glioblastoma multiforme; GCT, testicular germ cell tumor; HNSC, head & neck squamous cell carcinoma; KICH, kidney chromophobe; KIRC, kidney clear cell carcinoma; KIRP, kidney papillary cell carcinoma; LAML, acute myeloid leukemia; LGG, brain lower grade glioma; LIHC, liver hepatocellular carcinoma; LUAD, lung adenocarcinoma; LUSC, lung squamous cell carcinoma; MESO, mesothelioma; OV, ovarian serous cystadenocarcinoma; PAAD, pancreatic adenocarcinoma; PB, pulmonary blastoma; PCPG, pheochromocytoma & paraganglioma; PCPG, pheochromocytoma & paraganglioma; PitB, Pituitary blastoma; PRAD, prostate adenocarcinoma; PSC, Pulmonary sarcomatoid carcinoma; READ, rectum adenocarcinoma; SARC, sarcoma; SKCM, skin cutaneous melanoma; STAD, stomach adenocarcinoma; TGCT, testicular germ cell tumor; THCA, thyroid carcinoma; THYM, thymoma; TMB, tumor mutation burden; TPS, tumor proportion score; TUVM, uveal melanoma; UCEC, uterine corpus endometrioid carcinoma; UCS, uterine carcinosarcoma; UVM, uveal melanoma.

significantly high IGF2 expression in the patient. IGF2 imprinting aberration was proved to be the potential critical events to disease initiation in pancreatoblastoma[39] and hepatoblastoma.[45] IGF2 dysfunction was also intertwined with the progression of multiple malignant diseases.[46-50] Our results suggested that the IGF2 imprinting dysregulation was one of the important molecular mechanisms of PB pathogenesis.

Orthodoxly, PB is a subtype of PSC while they are still heterogeneous in pathological morphologies and clinical features. We introduced the multi-omics data of PSC (mainly pleomorphic PSC) and PitB into our study to explore the associations in the molecular characteristics among these malignancies. PB and PitB, in which we identified a high rate of *DICER1* mutations, exhibited higher levels of similarities in the mutational spectrum than PB and PSC. Moreover, by calculating the Euclidean distance-based similarities, we found that PB was more similar in DNA methylation profiles to PitB than to PSC. These results indicated that the organ heterogeneity between PB and PitB could not mask the inner associations, and it might be more suitable to take PB out of PSC in future basic research and clinical treatment.

PB remains an entity without effective treatment.[18,19,51,52] We identified PIK3CA and AKT1 missense mutations in 28.6 % and 14.3 % of patients, respectively. These mutations were within the PIK3CA kinase domain. According to previous studies, mutations in the PIK3CA kinase domain could activate the mitogen-activated protein kinase pathway and promote cell proliferation/transformation.[53] These suggested the potential applicability of PI3K inhibitors, such as alpelisibin,[54] in PB. The detection of AKT1 E17K mutation implies the application of AKT inhibitors, such as capivaseritib,[55] in PB, while their efficacy warrants further investigation.

Immunotherapy has revolutionized cancer treatment in the recent decade, but only a minority of patients derive long-term clinical benefits from ICIs. In our study, although the pan-cancer analysis showed that TMB and LF of PB were low, we found that one patient of our cohort was positive for PD-L1, and CD8-positive focal areas were detected in some

PB patients, implying the potential applicability of ICIs in PB. Generally, PB immunotherapy is at dawn, and investigation on large-scale cohorts is needed.

In summary, we provided a comprehensive molecular scenario of PB and deepened the public's understanding of the pathogenesis and therapeutic strategies of PB.

Declaration of competing interest

The authors declare that they have no known competing financial interests or personal relationships that could have appeared to influence the work reported in this paper.

Ethics statement

This study was performed in accordance with the local ethical regulations and the guidelines of the Declaration of Helsinki. The National Cancer Center/Cancer Hospital Ethics Committee, Chinese Academy of Medical Sciences, and Peking Union Medical College approved this study (approval number: 18–224/1782). Informed consent was obtained from each participant.

Data availability

WES and RNA-seq data have been deposited to Genome Sequence Archive (GSA) in Beijing Institute of Genomics (BIG) Data Center, under accession number HRA002783. The DNA methylation data have been deposited in OMIX in BIG Data Center, under accession number OMIX001595. A list of candidate somatic nonsynonymous mutations of PB was in Supplementary Table 2. All the other relevant data of the study are available from the corresponding authors upon reasonable request. Source data are provided in this paper.

Acknowledgments

We sincerely appreciate Dr. William D. Foulkes from the Department of Medical Genetics, Lady Davis Institute, Segal Cancer Centre, and Jewish General Hospital. He provided the methylation data of PitB to us for scientific research and gave us much academic support. The study was supported by National Natural Sciences Foundation (grant number: 82203827).

Author contributions

J.H. and Y.G. are responsible for the study design. H.T., Z.Y., J.Y., and Y.C. are responsible for conception identification. H.T., Z.Y., and Y.C. are responsible for data acquisition. J.Y. and H.T. are responsible for the analysis and interpretation of data. H.T. and Z.Y. are responsible for drafting the manuscript. L.L., T.F., T.L., and G.B. are responsible for revising the article critically for important intellectual content. J.H., Y.G., Z.Y., H.T., J.Y., and Y.C. provide the final approval of the version to be published. All authors read and approved the final manuscript. The work reported in the paper has been performed by the authors unless specified in the text.

Supplementary materials

Supplementary material associated with this article can be found, in the online version, at doi:10.1016/j.jncc.2024.12.001.

References

1. Bu X, Liu J, Wei L, Wang X, Chen M. Epidemiological features and survival outcomes in patients with malignant pulmonary blastoma: a US population-based analysis. *BMC Cancer*. 2020;20(1):811.
2. Robert J, Pache JC, Seium Y, de Perrot M, Spiliopoulos A. Pulmonary blastoma: report of five cases and identification of clinical features suggestive of the disease. *Eur J Cardiothorac Surg*. 2002;22(5):708–711.
3. Tsao MS, Nicholson AG, Maleszewski JJ, Marx A, Travis WD. Introduction to 2021 WHO Classification of Thoracic Tumors. *J Thorac Oncol*. 2022;17(1):e1–e4.
4. Macher-Goeppinger S, Penzel R, Roth W, et al. Expression and mutation analysis of EGFR, c-KIT, and β-catenin in pulmonary blastoma. *J Clin Pathol*. 2011;64(4):349–353.
5. Nakatani Y, Miyagi Y, Takemura T, et al. Aberrant nuclear/cytoplasmic localization and gene mutation of beta-catenin in classic pulmonary blastoma: beta-catenin immunostaining is useful for distinguishing between classic pulmonary blastoma and a blastomatoid variant of carcinosarcoma. *Am J Surg Pathol*. 2004;28(7):921–927.
6. Pelosi G, Gasparini P, Cavazza A, et al. Multiparametric molecular characterization of pulmonary sarcomatoid carcinoma reveals a nonrandom amplification of anaplastic lymphoma kinase (ALK) gene. *Lung Cancer*. 2012;77(3):507–514.
7. Sekine S, Shibata T, Matsuno Y, et al. Beta-catenin mutations in pulmonary blastomas: association with morule formation. *J Pathol*. 2003;200(2):214–221.
8. Zhao J, Xiang C, Zhao R, et al. Clinicopathologic features and genomic analysis of pulmonary blastomatoid carcinosarcoma. *BMC Cancer*. 2020;20(1):248.
9. Hill DA, Ivanovich J, Priest JR, et al. DICER1 mutations in familial pleuropulmonary blastoma. *Science*. 2009;325(5943):965.
10. Schultz KAP, Williams GM, Kamihara J, et al. DICER1 and Associated Conditions: identification of At-risk Individuals and Recommended Surveillance Strategies. *Clin Cancer Res*. 2018;24(10):2251–2261.
11. de Kock L, Bah I, Brunet J, et al. Somatic DICER1 mutations in adult-onset pulmonary blastoma. *Eur Respir J*. 2016;47(6):1879–1882.
12. Suzuki M, Kasajima R, Yokose T, et al. Comprehensive molecular analysis of genomic profiles and PD-L1 expression in lung adenocarcinoma with a high-grade fetal adenocarcinoma component. *Transl Lung Cancer Res*. 2021;10(3):1292–1304.
13. de Kock L, Bah I, Wu Y, Xie M, Priest JR, Foulkes WD. Germline and somatic DICER1 mutations in a well-differentiated fetal adenocarcinoma of the lung. *J Thorac Oncol*. 2016;11(3):e31–e33.
14. González IA, Stewart DR, Schultz KAP, Field AP, Hill DA, Dehner LP. DICER1 tumor predisposition syndrome: an evolving story initiated with the pleuropulmonary blastoma. *Mod Pathol*. 2022;35(1):4–22.
15. Yao G, Yang M, Wang S, He P, Wang J, Chen J. [Pulmonary blastoma: a report of five cases and review of the literature]. *Zhongguo Fei Ai Za Zhi*. 2005;8(2):132–135.
16. Luo Z, Cao C, Xu N, Ying K. Classic biphasic pulmonary blastoma: a case report and review of the literature. *J Int Med Res*. 2020;48(10):300060520962394.
17. Cutler CS, Michel RP, Yassa M, Langleben A. Pulmonary blastoma: case report of a patient with a 7-year remission and review of chemotherapy experience in the world literature. *Cancer*. 1998;82(3):462–467.
18. Mulamalla K, Truskinovsky AM, Dudek AZ. Pulmonary blastoma with renal metastasis responds to sorafenib. *J Thorac Oncol*. 2007;2(4):344–347.
19. Meng Z, Chen P, Zang F, et al. A patient with classic biphasic pulmonary blastoma harboring CD74-ROS1 fusion responds to crizotinib. *Onco Targets Ther*. 2018;11:157–161.
20. Yang Z, Xu J, Li L, et al. Integrated molecular characterization reveals potential therapeutic strategies for pulmonary sarcomatoid carcinoma. *Nat Commun*. 2020;11(1):4878.
21. de Kock L, Sabbaghian N, Plourde F, et al. Pituitary blastoma: a pathognomonic feature of germ-line DICER1 mutations. *Acta Neuropathol*. 2014;128(1):111–122.
22. Nadaf J, de Kock L, Chong AS, et al. Molecular characterization of DICER1-mutated pituitary blastoma. *Acta Neuropathol*. 2021;141(6):929–944.
23. Detterbeck FC, Boffa DJ, Kim AW, Tanoue LT. The Eighth Edition Lung Cancer Stage Classification. *Chest*. 2017;151(1):193–203.
24. Foulkes WD, Priest JR, Duchaine TF. DICER1: mutations, microRNAs and mechanisms. *Nat Rev Cancer*. 2014;14(10):662–672.
25. Vedanayagam J, Chatila WK, Aksoy BA, et al. Cancer-associated mutations in DICER1 RNase IIIa and IIIb domains exert similar effects on miRNA biogenesis. *Nat Commun*. 2019;10(1):3682.
26. Gao C, Wang Y, Broaddus R, Sun L, Xue F, Zhang W. Exon 3 mutations of CTNNB1 drive tumorigenesis: a review. *Oncotarget*. 2018;9(4):5492–5508.
27. Kim S, Jeong S. Mutation Hotspots in the β-Catenin Gene: lessons from the human cancer genome databases. *Mol Cells*. 2019;42(1):8–16.
28. Zhou F, Huang Y, Cai W, et al. The genomic and immunologic profiles of pure pulmonary sarcomatoid carcinoma in Chinese patients. *Lung Cancer*. 2021;153:66–72.
29. Lococo F, Torricelli F, Rossi G, et al. Inter-relationship between PD-L1 expression and clinic-pathological features and driver gene mutations in pulmonary sarcomatoid carcinomas. *Lung Cancer*. 2017;113:93–101.
30. Albrecht LV, Tejeda-Muñoz N, De Robertis EM. Cell biology of canonical wnt signaling. *Annu Rev Cell Dev Biol*. 2021;37:369–389.
31. Rim EY, Clevers H, Nusse R. The Wnt pathway: from signaling mechanisms to synthetic modulators. *Annu Rev Biochem*. 2022;91:571–598.
32. Soejima H, Higashimoto K. Epigenetic and genetic alterations of the imprinting disorder Beckwith-Wiedemann syndrome and related disorders. *J Hum Genet*. 2013;58(7):402–409.
33. Lopes MBS. The 2017 World Health Organization classification of tumors of the pituitary gland: a summary. *Acta Neuropathol*. 2017;134(4):521–535.
34. de Kock L, Priest JR, Foulkes WD, Alexandrescu S. An update on the central nervous system manifestations of DICER1 syndrome. *Acta Neuropathol*. 2020;139(4):689–701.
35. Reck M, Remon J, Hellmann MD. First-line immunotherapy for non-small-cell lung cancer. *J Clin Oncol*. 2022;40(6):586–597.
36. Souza RC, Peasley ED, Takaro T. Pulmonary blastomas: a distinctive group of carcinosarcomas of the lung. *Ann Thorac Surg*. 1965;1:259–268.
37. Schultz KAP, Rednam SP, Kamihara J, et al. PTEN, DICER1, FH, and their associated tumor susceptibility syndromes: clinical features, genetics, and surveillance recommendations in childhood. *Clin Cancer Res*. 2017;23(12):e76–e82.
38. de Kock L, Sabbaghian N, Druker H, et al. Germ-line and somatic DICER1 mutations in pineoblastoma. *Acta Neuropathol*. 2014;128(4):583–595.

39. Isobe T, Seki M, Yoshida K, et al. Integrated molecular characterization of the lethal pediatric cancer pancreatoblastoma. *Cancer Res*. 2018;78(4):865–876.
40. Nagae G, Yamamoto S, Fujita M, et al. Genetic and epigenetic basis of hepatoblastoma diversity. *Nat Commun*. 2021;12(1):5423.
41. Hubbard AK, Spector LG, Fortuna G, Marcotte EL, Poynter JN. Trends in international incidence of pediatric cancers in children under 5 years of age: 1988-2012. *JNCI Cancer Spectr*. 2019;3(1):pkz007.
42. López-Terrada D, Alaggio R, de Dávila MT, et al. Towards an international pediatric liver tumor consensus classification: proceedings of the Los Angeles COG liver tumors symposium. *Mod Pathol*. 2014;27(3):472–491.
43. Scholz B, Korn C, Wojtarowicz J, et al. Endothelial RSPO3 controls vascular stability and pruning through non-canonical WNT/Ca(2+)/NFAT signaling. *Dev Cell*. 2016;36(1):79–93.
44. Bugter JM, Fenderico N, Maurice MM. Mutations and mechanisms of WNT pathway tumour suppressors in cancer. *Nat Rev Cancer*. 2021;21(1):5–21.
45. Honda S, Arai Y, Haruta M, et al. Loss of imprinting of IGF2 correlates with hypermethylation of the H19 differentially methylated region in hepatoblastoma. *Br J Cancer*. 2008;99(11):1891–1899.
46. Fenner A. Prostate cancer: IGF2 imprinting loss promotes cancer. *Nat Rev Urol*. 2017;14(10):583.
47. Gao T, Liu X, He B, Pan Y, Wang S. IGF2 loss of imprinting enhances colorectal cancer stem cells pluripotency by promoting tumor autophagy. *Aging (Albany NY)*. 2020;12(21):21236–21252.
48. Sélénou C, Brioude F, Giabicani E, Sobrier ML, Netchine I. IGF2: development, Genetic and Epigenetic Abnormalities. *Cells*. 2022;11(12):1886.
49. Soroceanu L, Kharbanda S, Chen R, et al. Identification of IGF2 signaling through phosphoinositide-3-kinase regulatory subunit 3 as a growth-promoting axis in glioblastoma. *Proc Natl Acad Sci U S A*. 2007;104(9):3466–3471.
50. Lu L, Katsaros D, Wiley A, et al. The relationship of insulin-like growth factor-II, insulin-like growth factor binding protein-3, and estrogen receptor-alpha expression to disease progression in epithelial ovarian cancer. *Clin Cancer Res*. 2006;12(4):1208–1214.
51. Zagar TM, Blackwell S, Crawford J, et al. Preoperative radiation therapy and chemotherapy for pulmonary blastoma: a case report. *J Thorac Oncol*. 2010;5(2):282–283.
52. Lindet C, Vanhuyse M, Thebaud E, Robin YM, Penel N. Pulmonary blastoma in adult: dramatic but transient response to doxorubicin plus ifosfamide. *Acta Oncol*. 2011;50(1):156–157.
53. Arafeh R, Samuels Y. PIK3CA in cancer: the past 30 years. *Semin Cancer Biol*. 2019;59:36–49.
54. Savas P, Lo LL, Luen SJ, et al. Alpelisib monotherapy for PI3K-altered, pretreated advanced breast cancer: a Phase II study. *Cancer Discov*. 2022;12(9):2058–2073.
55. Turner NC, Oliveira M, Howell SJ, et al. Capivasertib in hormone receptor-positive advanced breast cancer. *N Engl J Med*. 2023;388(22):2058–2070.